

FATIGUE CHARACTERIZATION OF 3D PRINTED ELASTOMER MATERIAL

Jacob P. Moore and Christopher B. Williams

Design, Research and Education for Additive Manufacturing Systems Laboratory

Department of Mechanical Engineering

Virginia Polytechnic Institute and State University

REVIEWED, Accepted August 20, 2012

Abstract

The Objet PolyJet 3D Printing process provides the ability to print graded materials featuring both stiff and elastomeric polymers. This capability allows for a variety of new design possibilities for additive manufacturing such as living hinges, shock absorbing casings, and integrated gaskets. Such design features typically rely upon the ability of traditional elastomers to experience large and repeated strains without permanent deformation or damage. However, voids and other flaws inherent to many Additive Manufacturing (AM) processes can have a significant negative impact on the fatigue life of elastomeric AM materials. In this paper, the authors seek to fill a gap in the literature by characterizing the fatigue life of a direct 3D printed elastomer, and the multi-material interface. Based on the results, the authors offer advice for improving fatigue life of printed elastomeric components.

Keywords: Direct 3D Printing, Objet PolyJet, Elastomer, Fatigue

1. Background and Motivation

The Objet PolyJet process is a direct 3D printing process (direct 3DP) in which layers of photopolymer are printed onto the build platform via inkjet print heads. During printing, UV lamps (located on either side of the print head) cure the recently deposited photopolymer.

The direct 3DP process differs from the more common indirect 3DP processes in that the build material is being jetted, rather than jetting a binder into a bed of build material. Because there is no powder bed in direct 3DP processes, multiple materials can be printed in the same build – similar to the manner in which multiple colors can be printed with traditional inkjet printers.

Objet has developed a number of different photopolymers with differing degrees of stiffness, strength, and transparency. TangoBlackPlus a “rubber-like” photopolymer has the lowest Young’s Modulus (E) of any PolyJet material [1]. The ability to print elastomers such as TangoBlackPlus using the Objet PolyJet process, particularly the ability to print elastomers integrated with other stiffer materials, creates an opportunity for a variety of new design possibilities for additive manufacturing. Potential applications of 3D printed elastomers include

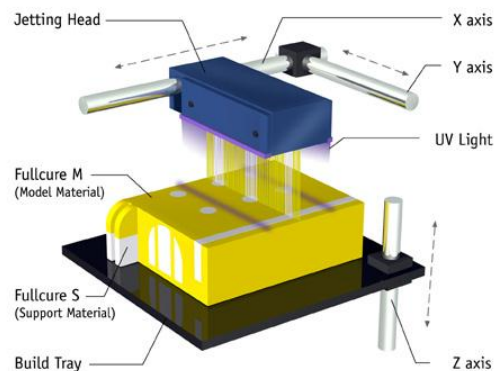


Figure 1: An illustration of the Objet direct 3DP process [1]



Figure 2: A 3DP part with elastomer living hinges (shown in black) [1]

integrated shock absorption components, integrated grips, living hinges, gaskets, and other flexible components that traditionally utilize the unique properties of elastomers. An example of a PolyJet part with integrated elastomer living hinges (the black material) is shown in Figure 2.

One of the key characteristics of traditional elastomers is their ability to experience large repeated strains without permanent deformation or failure. With Objet labeling these new materials as “rubber-like,” many designers may expect the material to exhibit the same abilities of traditional elastomers. However, the flaws and voids caused by the layer-by-layer fabrication process in many AM processes [2]

may significantly reduce the fatigue life of printed elastomers, since fatigue failure in elastomers is the result of the propagation of small tears present in the specimen due to manufacturing [3, 4]. As there is no data available on the fatigue characteristics of the TangoBlackPlus material, designers have no way to predict the lifetime of the elastomeric components of their product. This paper seeks to fill this gap in the literature by:

1. Determining the fatigue characteristics of the TangoBlackPlus material.
2. Determining the fatigue characteristics of the interface between TangoBlackPlus and another stiffer material (VeroWhitePlus).
3. Determine factors that may increase or compromise the fatigue life of the printed TangoBlackPlus material.
4. Offering design guidelines to improve the fatigue life of the printed elastomeric components.

To accomplish these goals, the authors first provide a review of the literature in Section 2, describe the experimental methodology in Section 3, present and discuss the results of the experiments in Section 4, and finally describe the implications of the results and discuss areas for further research in Section 5.

2. Literature Review and Theory

2.1 Fatigue in Printed Elastomers

The manufacturer does not offer any information on the fatigue properties of the printed elastomeric material [1]. Though information is available on the static material properties of TangoBlackPlus [1] and work has been done to model the static properties of direct 3DP materials [5, 6], a literature search did not reveal any research examining the fatigue characteristics of direct 3DP components.

Because no research thus far has examined the fatigue characteristics of printed elastomers, two bodies of literature were examined to better understand the theory applicable to fatigue failure in printed elastomers: (i) literature on the fatigue characteristics of traditionally manufactured elastomers and (ii) literature on the fatigue characteristics of non-elastomer AM

parts. Together it is hoped that the two bodies of literature will provide some insight into the fatigue behaviors of printed elastomers.

2.2 Fatigue in Traditionally Manufactured Elastomers

Because of the extensive use of rubbers in automobile tires, which experience high cycle loadings during regular use and pose a safety risk upon failure, the fatigue properties of many rubber compounds have been extensively examined. The tensile fatigue failure process in rubber as documented by the literature [3, 4], begins at small imperfections, usually located on the surface of the specimen that are introduced through the manufacturing process. These small imperfections cause local stress concentrations under loading. If stresses become large enough in these stress concentrations, some of the polymer chains can be mechanically broken, expanding the imperfection. Upon repeated loadings, the tear in the material is lengthened by a small amount each cycle until, at some point, the specimen experiences catastrophic tearing where the tearing rate increases substantially and complete part failure is the eventual result. Through this process, repeated cyclic exposure to loads significantly less than the maximum static load can result in complete part failure.

Below a given strain, typically less than 65% - 95% elongation for vulcanized rubbers, the elastomers can exhibit a fatigue limit [7]. Below this elongation, stress concentrations are not large enough to mechanically rupture the polymer chains around the part imperfections. This leads to a sharp jump in fatigue life, so long as the given strain is not exceeded in the cyclic loading. Parts experiencing cyclic loading below this limit do eventually experience complete part failure, but the primary driver is the chemical degradation of the material, rather than mechanical rupture of the polymer chains.

2.3 Fatigue in Non-Elastomeric AM Parts

There is some research on the fatigue properties of AM parts, but the literature is scarce. If a goal of the AM community is to use the technology as a manufacturing process, rather than just a prototyping tool, more research on the fatigue properties of AM components is needed. The existing research that was found on fatigue in AM components focuses on direct metal AM processes.

Studies have shown that if parts are sufficiently dense, and they are oriented to prevent delamination, the fatigue life of both plastic [8] and metal AM components [9, 10] can match their traditionally manufactured analogs. Different studies however have found that AM components have significantly shorter fatigue lives than their traditionally manufactured analogs [11, 12]. The presence of internal voids [9–12], and lamination weaknesses between build layers [8] in the AM components have been linked to premature fatigue failure of parts. Santos et al. inversely correlated the number of pores in metal AM specimens to the fatigue life of those specimens [12].

3. Methods

Following a review of the AM literature, it was found that no prior literature existed on the fatigue life of printed elastomers. To address this gap in the literature, the authors performed fatigue testing of multiple elastomeric specimens fabricated with the Objet Polyjet process. The methods used for this experiment are described in Section 3; the results of the experiment are presented in Section 4.

3.1 Specimen Creation Procedure

Because the printed elastomer is labeled as “rubber-like” by the manufacturer [1], the ASTM D4482-11 “Test Method for Rubber Property Extension Cycling Fatigue” [13] was used to guide the fatigue testing procedures for this study of the Objet TangoBlackPlus material.

The fatigue testing specimens were designed according to the ASTM standard and consisted of a modified dogbone shape. The exact dimensions of this shape can be seen in Figure 3. The specimen takes the shape of the traditional dogbone specimen with the addition of beaded edge, designed to fit into a set of special elastomer grips. This feature is necessary with elastomers because the lateral shrinkage of the specimens under high strains tends to let specimens pull out of traditional grips.

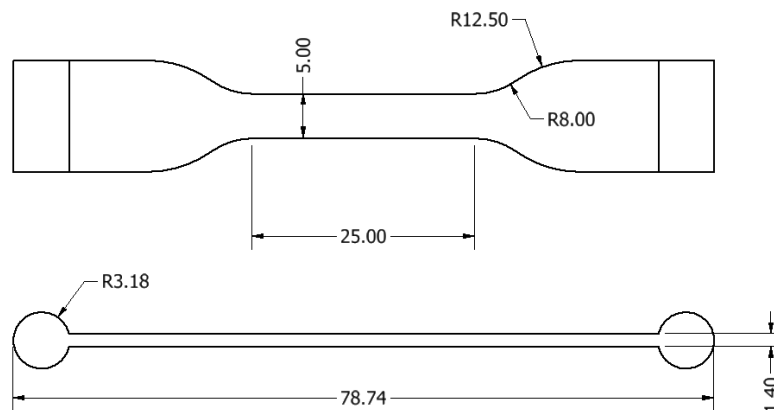


Figure 3: An engineering drawing of the fatigue test specimens. All measurements given in millimeters.

All specimens were printed on an Objet Connex 350 and cleaned of support material in a water-jet station. Specimens were printed with the TangoBlackPlus material in “digital material” mode (i.e., 32 μm layer thickness). The surface finish was set to the “matte finish” for all parts; thus, all surfaces were encased in support material. This ensured that the surface finish was consistent across all surface of the test specimens. The specimens were printed flat in the XY plane with the longest dimension of the part in the direction of the movement of the print carriage. Samples were positioned onto the build tray so as to ensure that all samples were printed with a single pass of the print head (per layer). Samples were positioned onto the build tray so as to ensure that all samples were printed with a single pass of the print head (per layer). This was done to ensure that all parts received uniform exposure from the UV lamp, (and therefore had uniform curing), since the differing UV exposure levels due to part spacing and part orientation can cause significant differences in part strength [14, 15].

To test the fatigue characteristics of the interface between the TangoBlackPlus material and a standard non-elastomer material (Objet's VeroWhitePlus, in this case) two alternate specimen designs were used: a flat interface specimen (Figure 4a) and a shear interface specimen (Figure 4b). Each of these specimens had the same overall part dimensions, but the specimens were made from the two materials.

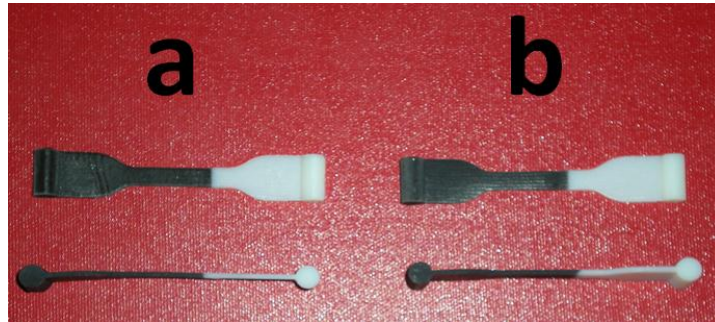


Figure 4: The flat interface and shear interface specimens

The flat interface specimen was intended to test the performance of the elastomer/non-elastomer interface under pure tensile loading. The interface between the VeroWhitePlus material and the TangoBlackPlus material was a flat plane normal to the direction of extension located in the reduced central region of the dogbone, five millimeters from the edge of the reduced central section. The interface was purposefully not centered, giving more area to the TangoBlackPlus, so that strain measurements could more accurately be made on the TangoBlackPlus material.

The shear interface specimen was intended to test the performance of the elastomer/non-elastomer interface under a combination of shear and tensile loading. Again, the interface was located in the reduced central region of the dogbone with five millimeters from the center of the interface to the edge. The interface was rotated by 45° from vertical, so that the interface plane would line up with the maximum shear plane in the specimen under extension.

3.2 Specimen Testing Procedure:

All specimens were printed and cleaned one day prior to testing to mitigate the effect of part ageing in this study. After cleaning, parts were allowed to dry overnight before testing.

Specimens were mounted and tested in an MTS Tytron 250 Microforce Testing System with a 250N load cell (Figure 5). The testing apparatus was chosen for its sensitivity to small loads and its large extension range. Special grips were designed and built on an FDM machine (from P-400 ABS material) to hold the beaded edge of the test specimens. The grips were adjusted until the load cell read between 0.05 and 0.1N of tension force in the specimen. This was set as the zero strain point for the specimen.



Figure 5: The MTS Tytron 250 Microforce Testing System

Because of delicate and non-rigid nature of the elastomer fatigue specimens, an extensometer could not be used to measure strain in the specimens. Instead, two small marks were painted onto the center section of the test specimen, at least two millimeters from the neck region of the specimen on either side. The distance between the inside edge of these two marks was measured with a set of calipers. The extension was then adjusted until the marks measured the appropriate reading for the desired maximum strain. The extension measurement and the force at the desired extension were then recorded. Pilot testing revealed that the relationship between extension and measured strain was very reliable across specimens, so the extension/strain coordination measurement was conducted only once at each desired level of strain for each type of fatigue specimen.

After the specimens were mounted and the maximum extension was determined for the desired strain, the specimens were tested in a loading and relaxation cycle until complete part failure. The loading and relaxation cycle was taken from the ASTM standard and consists of four phases. The standard specifies a testing frequency of 1.7 Hz, with four phases of equal length (each 0.147 sec). The phases are:

1. phase one consisted of hold at zero extension.
2. Phase two consisted of a linear ramp from zero extension up to the maximum extension.
3. Phase three consisted of a hold at the maximum extension.
4. A ramp down from the maximum extension to zero extension.

Figure 6 shows the commanded extension path and the actual extension part for one specimen during testing.

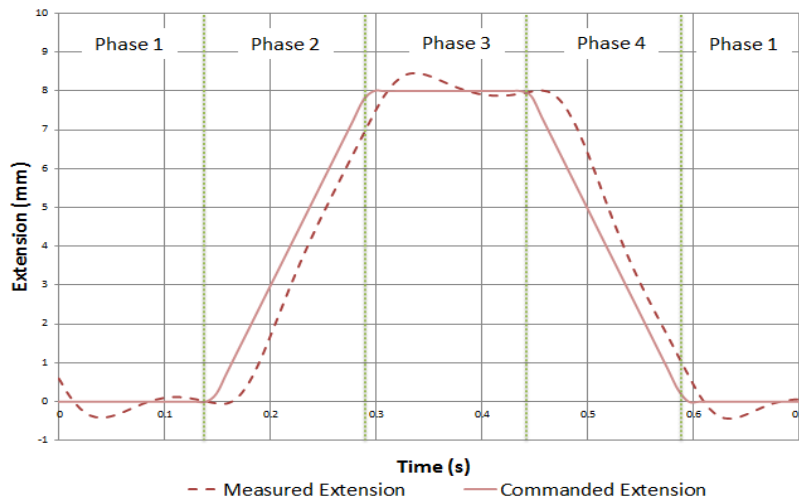


Figure 6: A plot of the fatigue extension cycle. In this example maximum extension is set to 8mm.

Complete part failure was defined as a complete rupture of the part, leaving the specimen in two pieces. Part failure was identified through an automated check of the tensile force at the beginning of phase three of the loading and relaxation cycle. If the tensile load during maximum extension fell below 0.1 N, the specimen was determined to have failed and the test was halted. The number of cycles was then rounded to the nearest integer and the cycles to failure for the given specimen was recorded.

4. Results and Discussion

4.1 Comparing the Fatigue Life of the Material and Multi-Material Interface

Before developing the ϵ -N curve, which relates the maximum strain (ϵ) to the expected material life in number of cycles (N), it was necessary to determine if the multi-material interface was weaker than the TangoBlackPlus material. Because the majority of example applications of TangoBlackPlus incorporate other materials interfacing with the TangoBlackPlus material [1], the fatigue characteristics of the multi-material interface were also of interest. It was hypothesized by the authors that the multi-material interface would fail under fatigue loading before the material itself failed. If this was true, the fatigue characteristics of the interface would be more valuable to the designer than the fatigue characteristics of the TangoBlackPlus material itself. To test this hypothesis, a comparison was carried out between test specimens made of only TangoBlackPlus, with no interface, and the flat interface specimens that did have a material interface.

To determine if the multi-material interface was in fact weaker than the TangoBlackPlus material, a set of twelve non-interface specimens was compared to a set of twelve flat interface specimens and statistical differences were examined in the fatigue life of those specimens. Extensions were set so that the TangoBlackPlus material located in the reduced central section of dogbone specimens experienced 40% elongation (a mid-range extension value identified in pilot testing). The results of this comparison are shown in Table 1.

Table 1: A comparison of specimens with and without a multi-material interface

Specimen Number	No Interface		Flat Interface	
	Cycles to Failure	Break Location	Cycles to Failure	Break Location
1	568	neck	1794	neck
2	1259	neck	1670	neck
3	1003	neck	1090	neck
4	787	neck	1122	neck
5	1158	neck	1299	interface
6	1226	neck	1184	neck
7	807	neck	1063	neck
8	1105	neck	1376	interface
9	841	neck	1388	neck
10	1020	neck	1740	neck
11	1617	neck	1289	neck
12	1367	neck	583	material

Mean Cycles to Failure 1063	Percentage Break at Neck 100%	Mean Cycles to Failure 1300	Percentage Break at Neck 75%
Standard Deviation 289		Standard Deviation 337	

P-value* = .078			
*Two tailed Students T-Test, no assumption of equal variance			

Contrary to the hypothesis, it was found that the interface specimens actually had a higher fatigue life than the non-interface specimens (though this difference was not statistically significant at the $p = 0.05$ level). Additionally, it was found that 100% of the non-interface specimens and 75% of the interface specimens failed at the necks made of TangoBlackPlus, rather than at the multi-material interface. Images of some of these specimens can be seen in Figure 7.

This finding led the authors to form a revised hypothesis that the TangoBlackPlus neck in the specimen was the weak point of the design. To test this new hypothesis, a new set of specimens with two multi-material interfaces was made. A drawing of these new specimens can be seen in Figure 8. With no necks made of the TangoBlackPlus material, a comparison of this new set of specimens to the existing two sets of specimens would allow the authors to compare specimens with and without necks made of the TangoBlackPlus material.



Figure 7: Pictures of the breaks at the TangoBlackPlus specimen neck

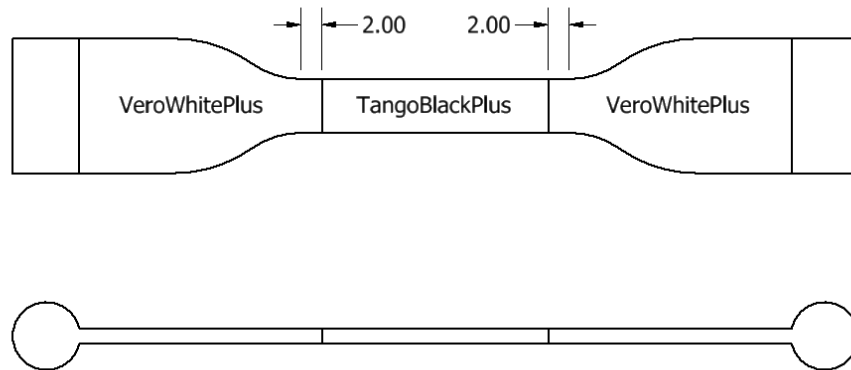


Figure 8: The Dual Interface Specimen

The extension for these new dual interface specimens was set so that the TangoBlackPlus materials experienced 40% elongation. Twelve specimens were tested at the 40% elongation level. These results are outlined in Table 2.

Table 2: The Dual Interface Specimens

Dual Interface	
Cycles to Failure	Break Location
32	interface
1345	material
1209	material
2128	material
1226	material
3491	interface
2588	material
2083	material
139	interface
1068	material
372	interface
250	interface

<p>Comparison of dual interface and no interface specimens p-value* = .426</p>
<p>Comparison of dual interface and no interface specimens p-value* = .933</p>
<p>*Two tailed Students T-Test, no assumption of equal variance</p>

Mean Cycles to Failure	Standard Deviation
1328	1076

As is seen in Table 2, the dual interface specimens had higher fatigue lives on average than both those with no interface and the single interface specimens (Table 1); however, neither of the differences are statistically significant. It can also be observed that the dual interface specimens seemed to have more variation in terms of the fatigue life. Finally, it was observed that 58% of the dual interface specimens failed in the central region (TangoBlackPlus), and not at either interface. Based on this data, there is no evidence to support the hypothesis that the multi-material interface has a fatigue life that is inferior to the TangoBlackPlus material's fatigue life.

4.2 Testing the Effects of Shear on the Interface

The multi-material interface was not found to have a shorter fatigue life than the TangoBlackPlus material under loading normal to the interface plane; however, this result was for a pure tensile loading of the interface. In application, the interface may be subjected to shear loading as well. To determine the effect of shear loading on the fatigue life of the specimen, another specimen was developed. This specimen was identical in design to the dual interface specimen, except one of the interfaces was angled 45° from vertical. This lined the interface up plane under the maximum shear force when the specimen was under elongation.

Twelve of these new shear specimens were created and compared to the original dual interface specimens. The extension for these new shear interface specimens was set so that the TangoBlackPlus materials experienced 40% elongation measured along the longer side of the TangoBlackPlus material. The results of this experiment are outlined in Table 3.

Table 3: Shear interface specimens

Shear Interface	
Cycles to Failure	Break Location
474	shear interface
500	shear interface
490	shear interface
585	shear interface
209	shear interface
733	shear interface
1221	shear interface
692	shear interface
1100	material
776	shear interface
855	shear interface
488	shear interface

Mean Cycles to Failure	Percentage Break at Shear Interface
677	92%

Standard Deviation	285
--------------------	-----

<p>Comparison of flat interface specimens to the shear interface specimens p-value* = .065</p>
<p>*Two tailed Students T-Test, no assumption of equal variance</p>

As is seen in Table 3, the introduction of the angled interface nearly halves the average fatigue life of the specimens. This difference is not statistically significant at the $p = 0.05$ level because of the large spread of the data, which is common in fatigue life analysis [16]. It can be observed that all but one of the shear specimens broke at the angled interface, indicating that the angled interface may indeed be the weakest point of the specimen.

4.3 Relating Material Strain to Expected Fatigue Life

Using the normal dual-interface specimens (Figure 8), which were identified as the most representative of the TangoBlackPlus material properties, the effect of maximum elongation on fatigue life was examined next. To relate these two variables, the authors sought to create a ϵ -N curve (also known as the Wöhler curve), to correlate material strain to expected fatigue life.

Twelve tests were conducted at each of the desired elongation ratios (20%**, 30%, 40%, 50% and 60%), to build this curve. The minimum value of 20% elongation was chosen because specimens were observed in pilot tests to have achieved fatigue lives of more than one million cycles at this extension ratio, which was an upper limit set on test duration set by the authors. The maximum of 60% elongation was chosen because specimens at 70% elongation regularly failed on the first elongation (indicating a maximum static elongation at break.)

A scatterplot of the data points can be seen in Figure 9. The break location of samples is indicated by the color of the point.

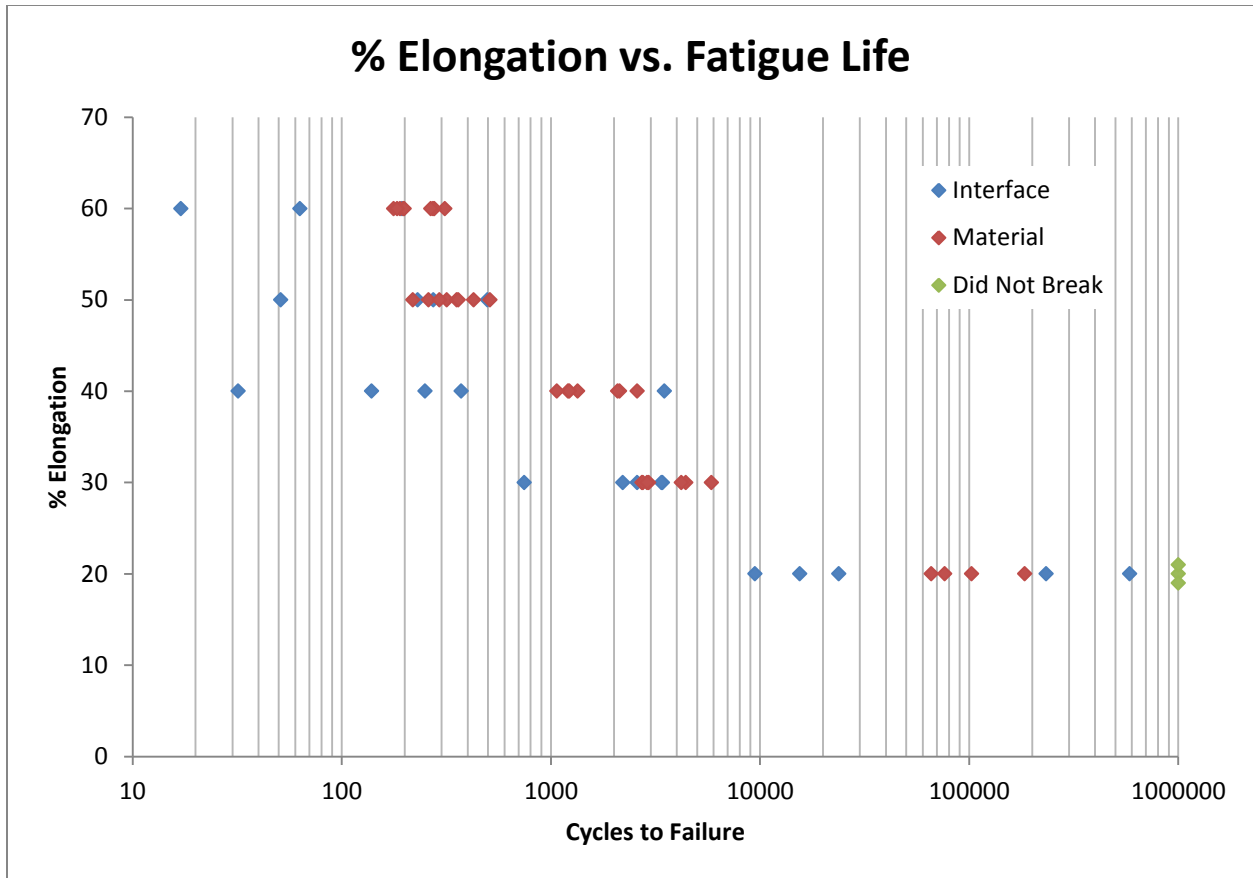


Figure 9: A scatterplot showing the relationship between material strain and fatigue life. Observed failure point indicated by color.

The scatterplot provides insights into the general shape of the ϵ -N curve, as well as the nature of the interface and the material. As can be seen in the data points, the specimens that failed in the material seem to have fatigue lives that are clustered fairly tightly around a central value. Alternatively, the fatigue lives of the specimens that broke at the interface are more erratic. The interface sometimes failed very prematurely, other times it did not fail at all (the material itself failed instead.)

A curve that predicts the fatigue life of a specimen for a given strain was constructed by averaging the scatter plot data of Figure 9, and is presented in Figure 10. The 95% confidence interval is denoted by the dashed lines in Figure 10.

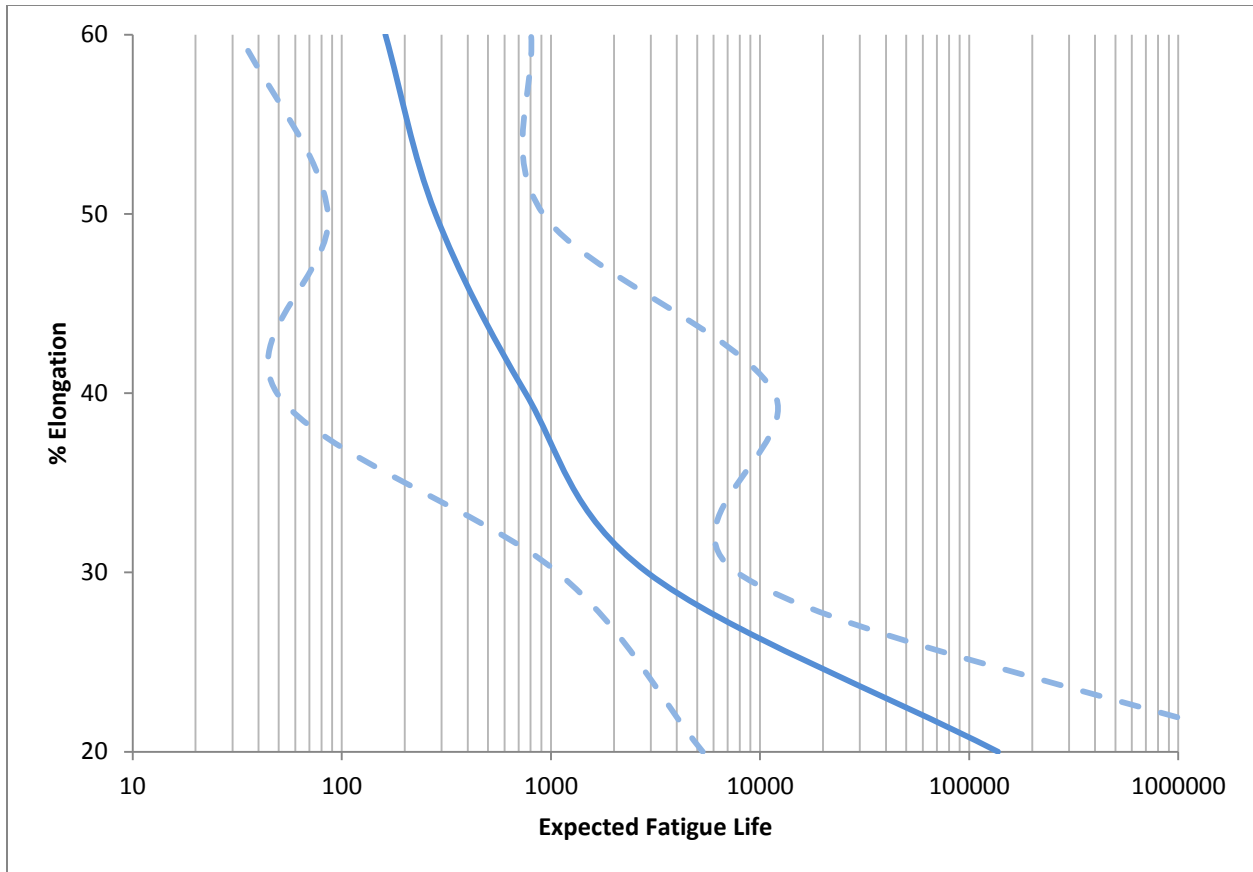


Figure 10: The ϵ -N curve for TangoBlackPlus. 95% CI denoted by the dashed lines.

Figure 10 gives designers a prediction on the fatigue life of their printed TangoBlackPlus component, based on the expected strain the material will experience. The confidence interval covers a very broad range, but this wide variability is a typical characteristic [16] of fatigue. Additionally, the erratic nature of the confidence interval is noteworthy. This is primarily due to the few very premature failures exhibited in the data (Figure 9). Elongation ratios that had more premature failures (such as 40% elongation) have wider variability, while elongation ratios that had only one or two premature failures (such as 30% elongation) have much less variability. With larger sample sizes, the erratic confidence interval would most likely be smoothed out.

5. Closure and Future Work

5.1 Conclusions

In this paper, the authors characterized the fatigue properties of a 3D printed elastomer (specifically, Objet's TangoBlackPlus). The findings are as follows:

- Contrary to the authors' hypothesis, the multi-material interface between elastomer and non-elastomer did not appear to have a shorter fatigue life than the material itself on average. This being said, there was some indication that the interface had more erratic fatigue behavior than the material, occasionally causing very premature fatigue failure.
- Reductions in in cross sectional area, such as the neck of the fatigue specimens, may cause serious reduction in fatigue life, even if the reductions are gradual.

- Shear forces on the multi-material interface have a negative impact on the fatigue life of the multi-material interface.
- A relationship between strain and fatigue life was found (Figure 10). Despite voids that are inherent to the 3DP process, the material specimens exhibited a long life at low extension ration (up to 10^6 cycles at 20% elongation)

5.2 Design Advice for Improving the Fatigue Life of Printed Elastomers

Based on the above conclusions, the authors offer the following suggestions for designers using 3D printed elastomers, in order to maximize the life of the elastomers their product.

1. Reduce the strain exerted on the elastomer. It was found that under low strains (20% elongation or less) the elastomers had a long fatigue life, approaching 10^6 cycles.
2. Avoid putting the elastomer/non-elastomer interface under shear loads. These shear loads will shorten the fatigue life of the multi-material interface.
3. Do not add necks to increase the area of the multi-material interface. This will not increase the design's life; it may in fact shorten the lifetime of the product.

5.3 Future Work

While this work provides insight into the fatigue characteristics of printed elastomers (e.g., fatigue life, material interface, interface geometry), there still remains opportunity for further research:

- What are the compressive fatigue characteristics of printed elastomers? This study only examined the tensile fatigue properties, a study that investigates compressive fatigue characteristics is needed.
- What is the effect of build orientation of the fatigue characteristics of printed elastomers? Only one build orientation (X-Y plane) was used in this study to simplify the analysis.
- What are the effects of surface finish on the fatigue life of printed elastomers? Different surface finish options may improve or harm the fatigue life of the material.
- What is the effect of part ageing the fatigue characteristics of printed elastomers? Past research has shown that photopolymers degrade with age [5].
- What is the effect of strain rate on the fatigue life of printed elastomers? Figure 11 shows an observed hysteresis effect with the fatigue specimens. This indicated a non-linearity in the stiffness of the material.

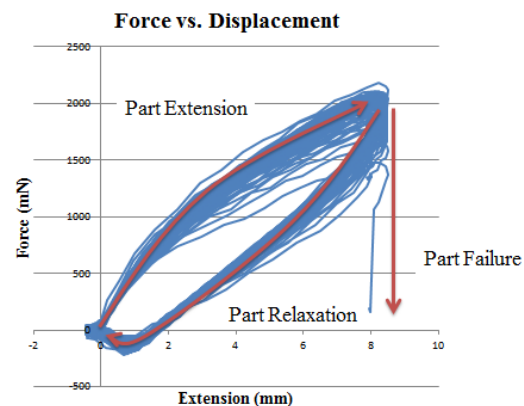


Figure 11: A plot showing the hysteresis effect in the TangoBlackPlus material

6. Acknowledgements

The authors would like to thank Nicholas Meisel for his help printing specimens, Dr. Dan Dudek for the use of his laboratory and the MTS Tytron 250, and Albert Kwansa for his expertise and help in using the MTS Tytron 250.

7. References

- [1] Objet Inc., “3D Printing & Rapid Prototyping by Objet Ltd,” *3D Printing & Rapid Prototyping by Objet Ltd*, 2012. [Online]. Available: <http://www.objet.com/>. [Accessed: 12-Jul-2012].
- [2] I. Gibson, D. W. Rosen, and B. Stucker, *Additive Manufacturing Technologies: Rapid Prototyping to Direct Digital Manufacturing*. Springer, 2009.
- [3] A. N. Gent, P. B. Lindley, and A. G. Thomas, “Cut Growth and Fatigue of Rubbers. I. The Relationship Between Cut Growth and Fatigue,” *Journal of Applied Polymer Science*, vol. 8, no. 1, pp. 455–466, 1964.
- [4] G. J. Lake and P. B. Lindley, “Cut Growth and Fatigue of Rubbers. II. Experiments on a Noncrystallizing Rubber,” *Journal of Applied Polymer Science*, vol. 8, no. 2, pp. 707–721, 1964.
- [5] I. Gibson, G. Goenka, R. Narasimhan, and N. Bhat, “Design Rules for Additive Manufacture,” 2010.
- [6] A. Pilipović, P. Raos, and M. Šercer, “Experimental Analysis of Properties of Materials for Rapid Prototyping,” *The International Journal of Advanced Manufacturing Technology*, vol. 40, no. 1, pp. 105–115, 2009.
- [7] G. J. Lake and P. B. Lindley, “The Mechanical Fatigue Limit for Rubber,” *Journal of Applied Polymer Science*, vol. 9, no. 4, pp. 1233–1251, 1965.
- [8] M. Blattmeier, G. Witt, J. Wortberg, J. Eggert, and J. Toepker, “Influence of Surface Characteristics on Fatigue Behaviour of Laser Sintered Plastics,” *Rapid Prototyping Journal*, vol. 18, no. 2, pp. 161–171, Feb. 2012.
- [9] B. Baufeld, E. Brandl, and O. van der Biest, “Wire Based Additive Layer Manufacturing: Comparison of Microstructure and Mechanical Properties of Ti–6Al–4V Components Fabricated by Laser-Beam Deposition and Shaped Metal Deposition,” *Journal of Materials Processing Technology*, vol. 211, no. 6, pp. 1146–1158, Jun. 2011.
- [10] F. Wang, “Mechanical Property Study on Rapid Additive Layer Manufacture Hastelloy (R) X Alloy by Selective Laser Melting Technology,” *International Journal of Advanced Manufacturing Technology*, vol. 58, no. 5–8, pp. 545–551, Jan. 2012.
- [11] E. Brandl, U. Heckenberger, V. Holzinger, and D. Buchbinder, “Additive Manufactured AlSi10Mg Samples Using Selective Laser Melting (SLM): Microstructure, High Cycle Fatigue, and Fracture Behavior,” *Materials & Design*, vol. 34, no. 0, pp. 159–169, Feb. 2012.
- [12] E. Santos, F. Abe, Y. Kitamura, K. Osakada, and M. Shiomi, “Mechanical Properties of Pure Titanium Models Processed by Selective Laser Melting,” in *Proceedings of the Solid Freeform Fabrication Symposium*, Austin, TX, 2002, pp. 180–186.
- [13] ASTM, “Test Method for Rubber Extension Cycling Fatigue,” Philadelphia, PA, Standard D4482-11, 2011.

- [14] M. Barclift and C. B. Williams, "Examining Variability in the Mechanical Properties of Parts Manufactured by Polyjet Direct 3D Printing," in *Proceedings of the Solid Freeform Fabrication Symposium*, Austin, TX, 2012.
- [15] A. Kęsy and J. Kotliński, "Mechanical properties of parts produced by using polymer jetting technology," *Archives of Civil and Mechanical Engineering*, vol. 10, no. 3, pp. 37–50, 2010.
- [16] J. A. Collins, *Mechanical Design of Machine Elements and Machines: A Failure Prevention Perspective*. Danvers, MA: John Wiley & Sons Inc, 2003.